JOC The Journal of Organic Chemistry

Article

pubs.acs.org/joc

Imidazoanthraquinone Derivatives for the Chromofluorogenic Sensing of Basic Anions and Trivalent Metal Cations

Cristina Marín-Hernández,[†,‡] Luis E. Santos-Figueroa,[†,‡] María E. Moragues,[†,‡] M. Manuela M. Raposo,*[,§] Rosa M. F. Batista,[§] Susana P. G. Costa,[§] Teresa Pardo,[†,‡] Ramón Martínez-Máñez,*[,†,‡] and Félix Sancenón[†,‡]

[†]Centro de Reconocimiento Molecular y Desarrollo Tecnológico (IDM), Unidad Mixta Universidad de Valencia-Universidad Politécnica de Valencia, Camino de Vera s/n, 46022 Valencia, Spain

[‡]CIBER de Bioingeniería, Biomateriales y Nanomedicina (CIBER-BBN)

[§]Centro de Química, Universidade do Minho, Campus de Gualtar, 4710-057 Braga, Portugal

Supporting Information

ABSTRACT: Four imidazoanthraquinone derivatives (**2a**−**d**) were synthesized and characterized and their coordination behavior against selected anions and cations tested. Acetonitrile solutions of probes showed charge-transfer absorptions in the 407−465 nm range. The four probes emitted in the 533−571 nm interval. The recognition ability of **2a**−**d** was evaluated in the presence of F^-, Cl^-, Br^-, I^-, OCN^-, BzO^-, ClO_4^-, AcO^-, HSO_4^-, $H_2PO_4^-$, and CN^-. Only F^-, AcO^-, and $H_2PO_4^-$ induced a new red-shifted absorption band that was attributed to a deprotonation process involving the amine moiety of the imidazole ring. Moreover, upon increasing quantities of F^-, AcO^-, and $H_2PO_4^-$, moderate quenching was induced in the emission of **2a**−**d** together with the appearance of a new red-shifted band. The UV−visible and emission behavior of the four probes in the presence of Cu^{2+}, Co^{2+}, Mg^{2+}, Fe^{3+}, Ba^{2+}, Fe^{2+}, Ni^{2+}, Ca^{2+}, Zn^{2+}, Pb^{2+}, Cd^{2+}, Cr^{3+}, Al^{3+}, K^+, and Li^+ was also assessed. Only addition of Fe^{3+}, Cr^{3+}, and Al^{3+} caused a new blue-shifted band in **2a**−**d** that was ascribed to a preferential coordination with the acceptor part of the probes. Moreover, an important quenching of the emission was observed which was ascribed to the interaction between these trivalent cations and **2a**−**d**.

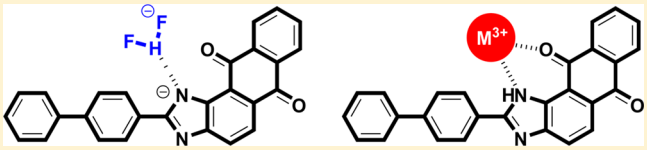

INTRODUCTION

The design of new molecular probes to detect anions, cations, and neutral species has gained primary significance in recent years due to the necessity to detect certain target analytes in environmental and biological samples.[1] In this context, these probes transform probe−analyte interactions into a signal which allows analyte detection via optical or electrochemical changes.[2] Among these particular output signals, optical responses are highly appealing due to the opportunity of using low-cost, extensively accessible instrumentation, and they offer, in certain circumstances, the possibility of detecting target species "to-the-naked-eye".[3] Moreover, chromofluorogenic chemosensors displaying a displacement of the absorption or emission band are of importance for the development of ratiometric procedures.[4] Optical detection probes for cations were developed before 20 years ago,[5] whereas the anionic ones have only been investigated during recent years.[6] In general, anion sensing is more challenging than cation detection. Comparing ions, anions usually show stability constants lower than those of metal cations, and some of them display a complex pH-dependence, and varied shapes, that make the design of selective receptors for anions more difficult than for cationic species.[7] However, despite these shortcomings, the design of anion probes has advanced and gained importance in recent years helped by the progress made in the understanding about the formation of host−anion complexes and how this knowledge can be used for the design of selective anion receptors.[8] The most widely approach to design probes is the use of the "binding site-signaling subunit" paradigm, in which the "'binding site"' is covalently connected to an optical "'signaling subunit"' in such a way that the interaction of certain species with the coordination site induces electronic modulations in the signaling unit, resulting in color or emission changes.[9] Inspired by these concepts, authors have designed a number of probes for anions using, in most cases, well-known binding interactions such as hydrogen bonding and electrostatic forces.[10,11]

Imidazole derivatives have been shown to be effective in coordinating anions.[12] Besides, acidity of the NH protons affects the hydrogen-bonding ability of the imidazole group. Its acidity can be modulated by the presence of easily delocalizable heteroaromatic rings, such as thiophene, pyrrole, and furan, electronically connected to the imidazole group, as a way to enhance intramolecular electronic delocalization.[13]

On the other hand, trivalent metal cations play crucial roles in biological processes, and their detection is a timely topic. For instance, iron is the most abundant transition metal in cellular

Received: July 14, 2014
Published: November 3, 2014

Scheme 1. Synthesis of Imidazoanthraquinone Receptors 2a−d

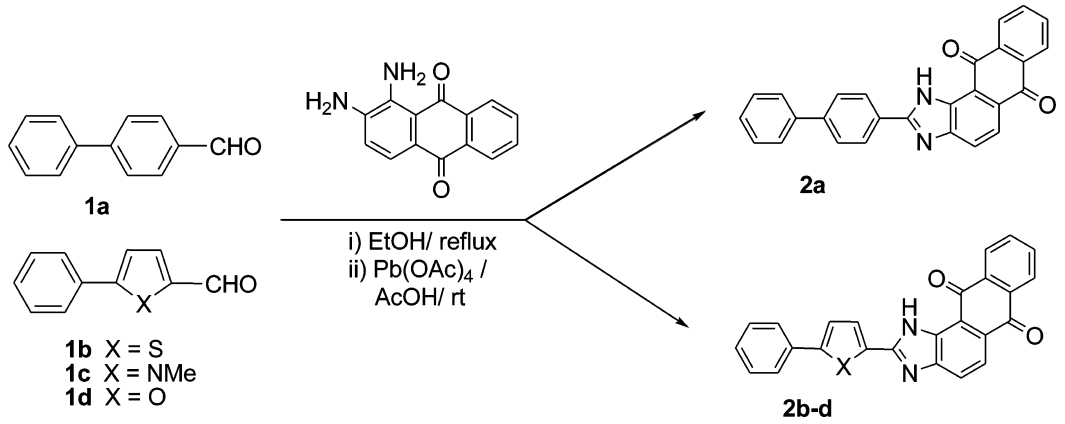

Table 1. Spectroscopic Data for the Interaction of 2a−d with Fluoride Anion

	absorbance data				fluorescence data				
	λ_{ab} LH (nm)	log ε	λ_{ab} L^- (nm)[a]	$\Delta\lambda_{ab}$ (nm)	λ_{ex} LH (nm)	λ_{em} LH (nm)	λ_{em} L^- (nm)[a]	$\Delta\lambda_{em}$ (nm)	Stokes shift (cm^{-1})
2a	407	4.25	479	72	438	544	588	44	6188
2b	435	4.30	490	55	465	571	608	37	5506
2c	465	4.22	514	49	458	533	609	76	3123
2d	441	4.13	501	60	467	568	621	53	4658

[a]Measured upon addition of 50 equiv of fluoride anion.

systems. More specifically, Fe^{3+} is an essential element in the growth and development of living systems as well as in many biochemical processes at the cellular level,[14] and its deficiency is associated with several diseases (anemia, hemochromatosis, diabetes, Parkinson's, and dysfunction of heart, pancreas, and liver).[15] On the other hand, aluminum is the third most abundant element in earth and the most abundant metallic element. Aluminum is highly used in several commercial applications such as water treatment, food additives, medicines, and metallic devices. Besides, some studies indicate that abnormal levels of aluminum ions in certain human tissues and cells could induce Alzheimer's and Parkinson's diseases.[16] Finally, Cr^{3+} is one of the most important nutrients in human and animal diet and plays a fundamental role in the metabolism of carbohydrates, proteins, lipids, and nucleic acids.[17] Its deficiency is associated with the development of diabetes and some cardiovascular diseases.[18] Moreover, its use in the metal industry has resulted in increased levels of chromium in the environment, and today has come to be regarded as a pollutant.[19]

From a different point of view, some anthraquinone derivatives have been recently reported as suitable systems for the colorimetric sensing of certain anions and have also been used for metal ion recognition.[20] Anthraquinones have been widely used in the manufacture of pigments,[21] fibers, and paper[22] in the textile industry[23] and of semiconductors in the electronic industry.[24] More recently, anthraquinones have attracted increasing research interest due to their bioactive properties, and some of their derivatives have been reported to be used as antiviral,[25] antibacterial,[26] antiparasitic,[27] insecticidal,[28] fungicidal,[29] antimalarial,[30] and anticancer agents.[31]

Taking into account the above-mentioned facts, and our interest in the development of optical probes,[32] we report herein the synthesis and characterization of a new family of imidazoanthraquinone derivatives functionalized with aromatic and heterocyclic groups (i.e., biphenyl, *N*-methylpyrrole, thiophene, and furan). The spectroscopic behavior of the designed probes in the presence of selected anions and cations was studied.

RESULTS AND DISCUSSION

Synthesis and Characterization. The formyl precursor **1c** was synthesized through Suzuki−Miyaura cross-coupling reaction of 1-methyl-2-(4,4,5,5-tetramethyl-1,3,2-dioxaborolan-2-yl)-1*H*-pyrrole with bromobenzene in dry DME with $Pd(PPh_3)_4$ as catalyst and Na_2CO_3, followed by Vilsmeier formylation. The new imidazoanthraquinone derivatives **2a−d** with biphenyl, phenylthiophene, phenylpyrrole, and phenylfuran substituents as π-conjugated groups were synthesized in moderate to good yields (32−71%). In a typical synthesis, aldehydes **1a−d** and 1,2-diaminoanthraquinone were heated for 15 h in ethanol at reflux using formic acid as catalyst, to yield the respective imines that were subsequently cyclized to the corresponding imidazoanthraquinones **2a−d** in the presence of lead tetraacetate in acetic acid as solvent and at room temperature (see Scheme 1). For all reactions, the crude products were purified by column chromatography on silica with chloroform or through recrystallization with dichloromethane to finally give the pure compounds. The four **2a−d** receptors were characterized by ^1H, ^{13}C NMR, and HRMS. The obtained data are in agreement with the expected structures (see Supporting Information and Experimental Section for details).

One of the most relevant characteristics in the ^1H NMR spectrum of this group of imidazoanthraquinone derivatives was that corresponding to N−H protons of the imidazole heterocycle which appeared as singlets downfield in the 12.74−13.38 ppm range. These values suggested the formation in solution of an intramolecular hydrogen bond between the NH of the imidazole ring and the neighboring quinone carbonyl group.[33]

dx.doi.org/10.1021/jo501515e | J. Org. Chem. 2014, 79, 10752−10761

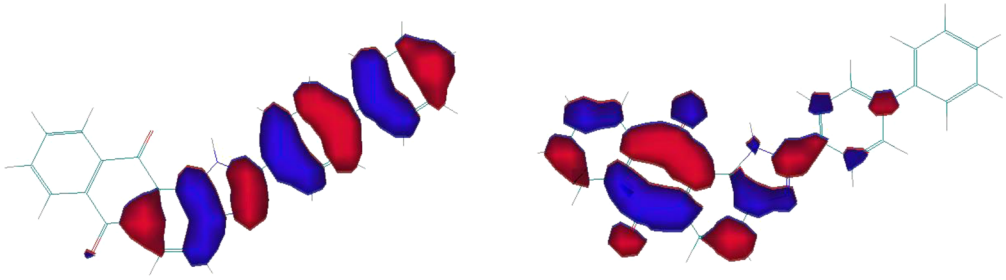

Figure 1. HOMO (left) and LUMO (right) orbitals for probe **2a**.

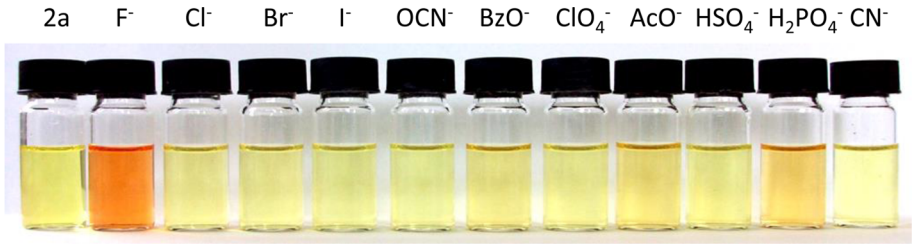

Figure 2. Color changes observed for probe **2a** (1.0×10^{-4} mol dm^{-3} in acetonitrile) upon addition of 10 equiv of the selected anions.

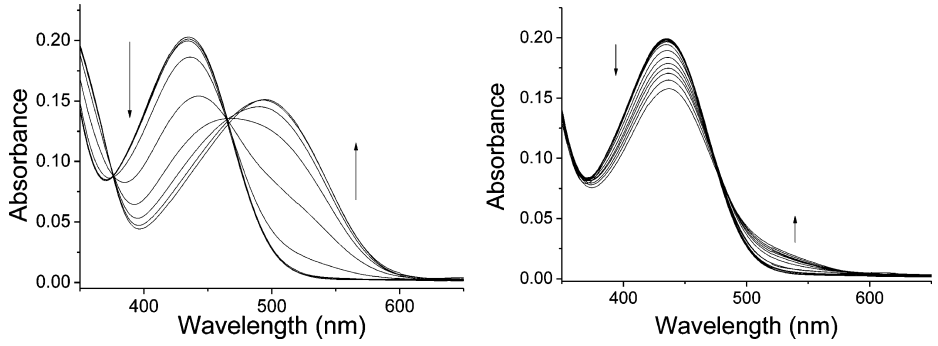

Figure 3. UV−vis titration profiles of receptor **2b** (1.0×10^{-5} mol dm^{-3} in acetonitrile) obtained upon the addition of F^- (left) and AcO^- (right) anions.

Spectroscopic Characterization. Acetonitrile solutions of imidazoanthraquinone derivatives **2a−d** presented a strong absorption (log $\varepsilon \approx 4.2$) in the 400−470 nm interval (see Table 1). The position of the visible absorption band in the receptors was clearly related to the electron donor strength of the aromatic or heterocycle system (pyrrole ≫ furan > thiophene > benzene) used as π-bridge linked to the imidazoanthraquinone moiety. In particular for **2a**, bearing a benzene π-bridge, the absorption band was centered at 407 nm. Upon changing the π-bridge to thiophene (**2b**) and furan (**2d**), the absorption maximum suffered a moderate bathochromic shift to 435 and 441 nm, respectively. Moreover when a *N*-methylpyrrole was used as a π-bridge (**2c**), the probe displayed a significant bathochromic shift to 465 nm. Additionally, upon excitation in the corresponding wavelength maximum for the four probes, a broad unstructured emission in the 540−580 nm region appeared (see Table 1).

The HOMO and LUMO differences in energy for probes **2a−d** were determined by quantum chemical studies at the semiempirical level using the PM3 model and with RMS gradient of 0.001. For the four receptors, the HOMO orbitals are mainly situated in the imidazole moiety and the heterocyclic rings (donor part of the molecule), whereas the LUMO orbitals are located in the anthraquinone moiety (acceptor fragment common to the four probes). These data indicated that the electronic transition between the HOMO and the LUMO has a charge-transfer character. As an example, Figure 1 shows the HOMO and LUMO orbitals for probe **2a**.

Spectroscopic Behavior of 2a−d in the Presence of Anions. In a first step, the ability of receptors **2a−d** to detect anions was studied. In typical experiments, the UV−vis spectrum of the probes was monitored in acetonitrile solutions at 25 °C in the presence of chosen anions of different sizes and shapes (i.e., F^-, Cl^-, Br^-, I^-, OCN^-, BzO^-, ClO_4^-, AcO^-, HSO_4^-, $H_2PO_4^-$, and CN^-). The chromogenic response observed with compounds **2a−d** was quite similar, and in all cases only addition of F^-, AcO^-, and $H_2PO_4^-$ anions induced color changes that were especially visible to the naked eye in the presence of F^- anion. As an example, Figure 2 shows the color modulations observed for probe **2a** upon addition of 10 equiv of selected anions.

As shown in Figure 2, acetonitrile solutions of probe **2a** were yellow and turned orange upon addition of F^- anion. Upon addition of AcO^- and $H_2PO_4^-$ anions, a moderate color change from yellow to dark yellow occurred. Other anions were unable to induce remarkable color changes. A similar behavior was observed for probes **2b**, **2c**, and **2d**; i.e., clear color modulations in the presence of F^- and only a moderate color change in the presence of AcO^- and $H_2PO_4^-$ anions.

dx.doi.org/10.1021/jo501515e | *J. Org. Chem.* 2014, 79, 10752−10761

Once the responses for **2a–d** probes toward anions were assessed, changes in the UV–visible spectrum in the presence of F^-, AcO^-, and $H_2PO_4^-$ were studied in more detail. UV–visible titration profiles of probe **2b** with F^- and AcO^- anions are shown in Figure 3 as an example. Acetonitrile solutions of probe **2b** displayed an intense band at 435 nm that, upon addition of increasing quantities of F^- anion, decreased in intensity while a new red-shifted band grew at 490 nm. In contrast, the addition of AcO^- and $H_2PO_4^-$ anions induced only moderate changes in the UV–visible profiles of probe **2b**. As shown in Figure 3, addition of increasing amounts of AcO^- anion resulted in a hypochromic effect for the band at 435 nm together with the appearance of a broad shoulder centered at ca. 520 nm. Similar titration profiles were obtained for $H_2PO_4^-$ anion and **2b**.

UV–visible titration experiments carried out with probes **2a**, **2c**, and **2d** showed the same behavior as that observed for **2b**, i.e., only the addition of F^- anion caused a remarkable decrease in the visible band of the receptor with a concomitant clear increase of a new red-shifted absorbance (see Supporting Information). Addition of AcO^- and $H_2PO_4^-$ anions to acetonitrile solutions of **2a**, **2c**, and **2d** induced small changes in the UV-profiles, similar to those depicted in Figure 3 for **2b** (data not shown).

The fact that color modulations in the four probes were induced by the addition of basic anions (F^-, AcO^-, and $H_2PO_4^-$) pointed to a ground-state proton shift as the mechanism for the chromogenic response observed.[34] In this scenario, addition of F^- anion would induce the deprotonation of the N–H moiety of the imidazoanthraquinone fragment, which is common to all four probes. The mechanism of the chromogenic response was assessed with additional titration experiments carried out with probes **2a–d** and tetrabutylammonium hydroxide that showed an identical behavior to that found in the presence of F^- anion (see Supporting Information). On the whole, the results were in agreement with the expectation that the deprotonation of a donor group in a push–pull system by an electron-rich anion would be expected to induce a bathochromic shift of the absorption band. Indeed, other benzimidazole-, urea-, thiourea-, amide-, pyrrole-, benzimidazole-, or thiosemicarbazone-containing probes have been reported to cause similar shifts upon addition of fluoride.[35] Besides, AcO^- and $H_2PO_4^-$ showed a less relevant response with the probes as expected because they are not as basic as F^- anion.[36] One striking feature of probes **2a–d** is their lack of response upon addition of the basic and nucleophilic CN^- anion. However, this lack of response has also been described in other anthraquinone-containing probes.[37]

The chromogenic behavior of **2a–d** toward F^- was rather selective, and for instance the intensity of the red-shifted absorption band obtained upon addition of 10 equiv of this anion is identical to that obtained in mixtures containing 10 equiv of fluoride and 10 equiv of Cl^-, Br^-, I^-, OCN^-,BzO^-, ClO_4^-, HSO_4^-, and CN^- anions (see Figure 4). Besides, the limits of detection of **2a–d** for F^- were also determined from the corresponding titration profiles. The values obtained were quite similar for the four probes and around 10 μM.

Once the UV–visible behavior of **2a–d** probes was assessed, more detailed fluorogenic studies with F^- anion were carried out. F^- was selected because this was the anion that induced the most remarkable changes in the UV–visible of the four probes. Emission titrations were carried out in acetonitrile solutions in the presence of F^- and using as λ_{ex} the corresponding isosbestic point observed in the UV–visible titrations. The obtained response with the four probes was quite similar and, as an example, Figure 5 shows the emission changes for probe **2a** upon addition of increasing quantities of F^-. As shown, probe **2a** showed a broad emission band at 544 nm (λ_{ex} = 438 nm), the intensity of which gradually decreased as the amount of F^- anion increased. Together with this quenching effect, a progressive bathochromic shift of the fluorescence was observed (from 544 to 588 nm upon addition of 2 equiv) with an isoemissive point at 576 nm.

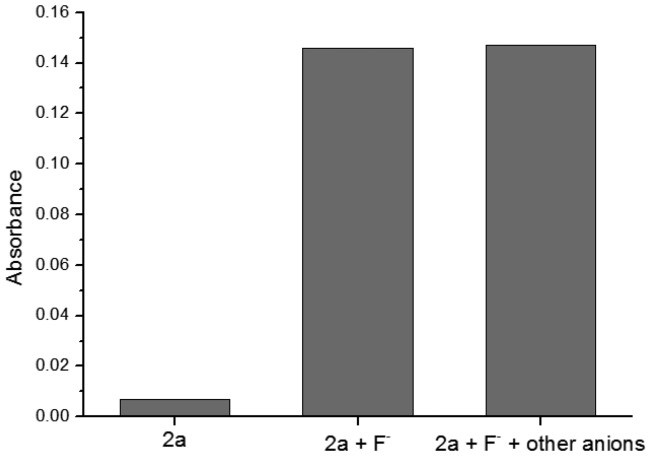

Figure 4. Absorbance of receptor **2a** (1.0×10^{-5} mol dm^{-3}) at 479 nm alone and upon the addition of 10 equiv of F^- anion and 10 equiv of Br^-, Cl^-, I^-, OCN^-, BzO^-, ClO_4^-, HSO_4^-, and CN^- anions in acetonitrile.

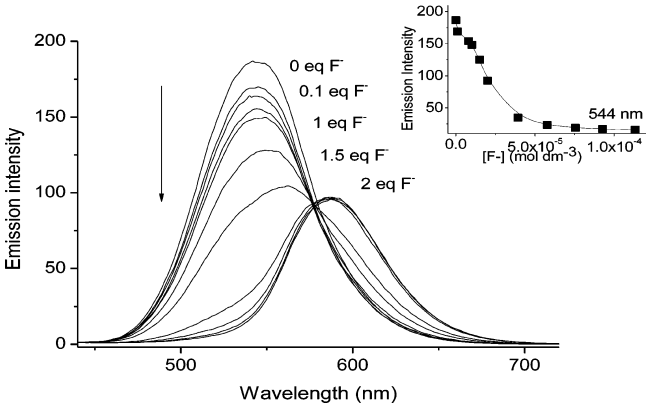

Figure 5. Emission spectra of probe **2a** (1×10^{-5} mol dm^{-3}) in acetonitrile upon addition of increasing quantities of F^- anion (excitation at 438 nm). The inset shows the change in the intensity of the 544 nm band upon addition of increasing quantities of F^- anion.

As a general trend, the remaining probes **2b–d** also showed a moderate bathochromic shift and a simultaneous partial quenching of their original emission band upon addition of increasing quantities of F^- anion. However, a more detailed look at the titration experiments indicated that, to induce the same behavior, larger amounts of fluoride were necessary for receptor **2b**, **2c**, and **2d** than for receptor **2a**. Emission data of the four probes alone and in the presence of F^- anion are shown in Table 1.

The emission changes observed for the four probes in the presence of F^- anion were quite similar to those observed for related derivatives.[38] For **2a–d**, the quenching of the initial

dx.doi.org/10.1021/jo501515e | J. Org. Chem. 2014, 79, 10752–10761

Table 2. Logarithms of the Stability Constants Measured for the Interaction of Probes 2a−d with F^- Anion

	2a	2b	2c	2d
log K	4.208 ± 0.006	3.308 ± 0.007	3.819 ± 0.071	3.381 ± 0.071

fluorescence band together with the appearance of the red-shifted emission was ascribed to a proton transfer process that yielded the deprotonated probes. This mechanism was proposed, for instance, by Han and co-workers for the interaction of fluoride with phenyl-1*H*-anthra(1,2-*d*)imidazole-6,11-dione, a probe closely related to **2a−d**.[39] The four probes alone are highly emissive. In the excited state, fluoride anion induced the loss of the proton of the N−H group, and the formed HF binds, through the formation of a weak hydrogen bond, with the deprotonated receptor. This complex is not stable; as a consequence, a deprotonation process takes place and the formed complex loses the HF molecule, yielding the also emissive anionic form of the corresponding probe. The lifetimes of the hydrogen bonded complexes are too short and are not observed experimentally in the emission titration profiles. The negative charge generated upon the proton transfer process induced a new emission band that corresponds to the deprotonated form which emits at a wavelength longer than that of the neutral probe.

The optical response of **2a−d** was also studied in mixed acetonitrile:water solutions. However, it was found that addition of more than 2% of water to acetonitrile disabled the chromofluorogenic response observed upon addition of F^- anion. This could be ascribed to the fact that F^- has a high free energy of solvation (−465 kJ mol^{-1}) and hence a strong affinity for coordinating water molecules rather than the N−H moiety of the four probes. The formation of a dense water shell around fluoride anion decreased significantly its basicity and, as a consequence, the proton transfer process was disabled.

Determination of Stability Constants with Anions and Quantum Mechanical Studies. As stated above, basic anions (such as F^-, AcO^-, and $H_2PO_4^-$) induced proton transfer processes in the probes **2a−d**. This proton transfer equilibrium is represented in eq 1 in which LH is the probe and A^- represents a basic anion such as fluoride.

$$LH + 2A^- \leftrightarrows L^- + A_2H^- \quad (1)$$

To complete the characterization of the interaction among **2a−d** with anions, the deprotonation process was studied by the determination of the stability constants from UV−vis spectroscopic titrations, using the HypSpec software.[40] The studies were performed using F^- because this was the anion that induced the most remarkable changes in the UV−visible (vide ante). The results are shown in Table 2.

The logarithms of the stability constants for probes **2b**, **2c**, and **2d** in their interaction with F^- were rather similar and lower than log K = 4. Moreover, when the π-bridge was a biphenyl system, the acidity of the N−H moiety was enhanced (pK of 4.208). This observed enhancement was clearly related to the lower electron donor character of the benzene ring, when compared with the pyrrole (**2c**), furan (**2d**), and thiophene (**2b**) heterocycles. Despite this fact, the logarithms of the stability constants for the proton transfer reactions for probes **2a−d** are of the same order of magnitude and similar to those reported for related compounds.[41]

It has been reported that the hydrogen bond-donating or -accepting ability of a molecule can be studied from quantum chemical calculations as a difference between the energy of the molecule and that of the deprotonated form.[13] Calculations for probes **2a−d** (assuming that the N−H moiety of the four receptors was deprotonated) were carried out using a PM3 semiempirical model, and the results are shown in Table 3.

Table 3. Stabilization Energy of the Deprotonation for Probes 2a−d

receptor	$E_{(LH)}$ (kcal/mol)	$E_{(L^-)}$ (kcal/mol)	$E_{(LH)} - E_{(L^-)}$ (kcal/mol)
2a	−5735.5	−5724.9	−10.6
2b	−5343.6	−5336.0	−7.6
2c	−5725.9	−5721.9	−4.0
2d	−5374.3	−5365.8	−8.5

Data in Table 3 indicated that the most acidic probe was **2a**. This was in agreement with the stability constants calculated above for the deprotonation process of the probes in the presence of fluoride. However, for the remaining chemosensors, there was not a clear correlation between the acidity predicted by quantum chemical calculations (i.e., **2d** > **2b** > **2c**) and that found from titration experiments (i.e., **2c** > **2d** > **2b**). This is most likely due to the different conditions in which the calculations were performed (gas for quantum calculations vs acetonitrile solutions for stability constants).

Spectroscopic Behavior of 2a−d with Cations. Probes **2a−d** contain in their structures two oxygen and two nitrogen atoms that could be able to coordinate with transition metal cations.[42] For this reason, the interaction of probes **2a−d** with selected cations (Cu^{2+}, Co^{2+}, Mg^{2+}, Fe^{3+}, Ba^{2+}, Fe^{2+}, Ni^{2+}, Ca^{2+}, Zn^{2+}, Pb^{2+}, Cd^{2+}, Cr^{3+}, Al^{3+}, K^+, and Li^+) in acetonitrile was studied upon addition of 10 equiv of the corresponding cation. Only addition of trivalent cations (Fe^{3+}, Al^{3+}, and Cr^{3+}) induced color changes in the acetonitrile solutions of the four probes.

Once the selective chromogenic response of **2a−d** to trivalent cations was assessed, more detailed studies of the four probes with Fe^{3+}, Al^{3+}, and Cr^{3+} were performed via UV−visible titrations. As a general trend, addition of increasing amounts of these cations induced a progressive reduction in absorption of the visible band concomitant with the growth of a new blue-shifted band. As an example of this behavior, Figure 6 shows the UV−visible titration profile of probe **2a** with Fe^{3+} cation. The absorption at 407 nm progressively decreased when increasing quantities of Fe^{3+} cation were added. At the same time, a new absorption band at 371 nm ($\Delta\lambda$ = 36 nm) was formed. These changes were reflected in a color modulation from yellow to colorless.

The emission behavior of **2a−d** in the presence of trivalent cations was also studied. The four probes presented a very similar response upon addition of Fe^{3+}, Al^{3+}, and Cr^{3+} cations, namely a marked emission quenching. As an example, Figure 7 shows the titration obtained for probe **2a** and Fe^{3+} cation. As shown, the emission at 543 nm (λ_{ex} = 396 nm) was progressively quenched upon addition of increasing amounts of Fe^{3+}. Changes in the UV−visible and emission of probes **2a−d** in the presence of trivalent cations are summarized in Table 4. Furthermore, the limits of detection of the four probes toward trivalent metal cations were evaluated from fluorescence

dx.doi.org/10.1021/jo501515e | J. Org. Chem. 2014, 79, 10752−10761

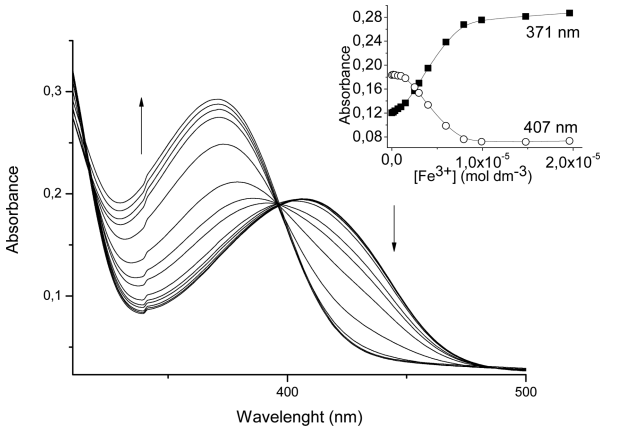

Figure 6. UV−visible titration of probe **2a** (1.0×10^{-5} mol dm^{-3}) with Fe^{3+} in acetonitrile. The inset shows the absorbance changes at 371 and 407 nm vs Fe^{3+} concentration.

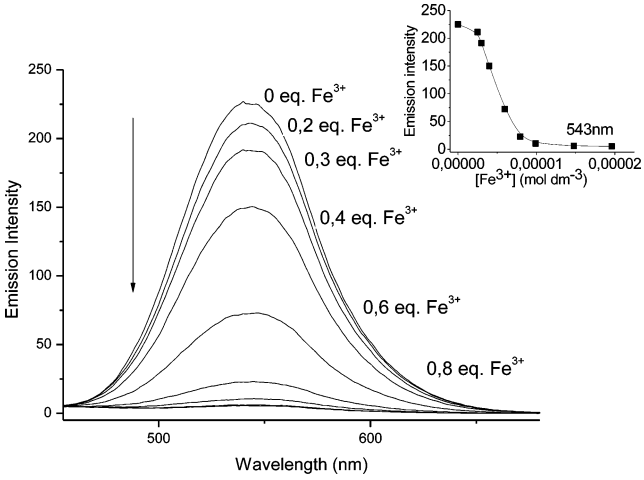

Figure 7. Emission spectra (excitation at 396 nm) of receptor **2a** (1.0×10^{-5} mol dm^{-3}) in acetonitrile upon addition of increasing quantities of Fe^{3+} cation. The inset shows the changes in the emission intensity at 543 nm vs Fe^{3+} concentration.

Table 4. Spectroscopic Data for Probes 2a−d with Trivalent Cations

	absorption wavelength (nm)				emission wavelength (nm)[a]			
receptor	LH	LH-Al^{3+}	LH-Cr^{3+}	LH-Fe^{3+}	LH	LH-Al^{3+}	LH-Cr^{3+}	LH-Fe^{3+}
2a	407	371	372	371	544	544	543	543
2b	435	410	410	410	571	559	562	563
2c	465	429	429	428	533	533	534	534
2d	441	419	419	419	580	558	556	555

[a]Measured upon excitation at isosbestic point in the UV−vis titration.

titration profiles. The values obtained were quite similar for all **2a−d** probes and are shown in Table 5.

The blue shift of the visible band of **2a−d** observed upon addition of trivalent cations was indicative of a preferential coordination with the donor part of the probes.[43] In fact, the results are in agreement with the expectation that the interaction between an electron-acceptor cation and a donor group in a push−pull system will induce a blue shift. The common donor fragment in the four probes is the imidazo group, and the results strongly suggested an interaction of the metal cations with this moiety.

Table 5. Limits of Detection for 2a−d Probes to Trivalent Cations (μM) from Emission Titrations

receptor	Fe^{3+}	Al^{3+}	Cr^{3+}
2a	1.43	1.78	0.98
2b	2.10	2.46	3.10
2c	1.65	–	1.89
2d	1.81	1.35	1.85

^{1}H NMR Spectroscopic Studies in the Presence of Cations. To study, in more depth, the coordination mode of probes **2a−d** with trivalent cations, ^{1}H NMR titration experiments were performed. For this purpose, we selected receptor **2a**, and changes in ^{1}H NMR spectra (in CD_3CN) upon addition of increasing quantities of Al^{3+} cation were studied.

The ^{1}H NMR spectrum of **2a** in CD_3CN (see Figure 8 for proton assignation) showed the signals of the monosubstituted benzene ring centered at 7.45 (t, Ha), 7.53 (t, Hb), and 7.80 (d, Hc) ppm. Protons of the 1,4-disubstituted benzene ring appeared at 7.90 (m, Hd overlapped with Hi) and at 8.38 (He) ppm whereas protons of the anthraquinone moiety appeared at 7.90 (m, Hi overlapped with Hd), 8.13 (d, Hf), 8.21 (d, Hg), and 8.31 (dd, Hh) ppm. As a general trend, addition of Al^{3+} cation induced downfield shifts of the signals of probe **2a** (see Figure 8). Besides, the shifts of the proton resonances stopped upon addition of 1 equiv of Al^{3+} cation, suggesting the formation of 1:1 (probe−cation) complexes.

The more remarkable shifts observed upon Al^{3+} addition were those of protons Hd, Hf, Hg, and He that are located in the 1,4-disubstituted benzene ring of the biphenyl system and in the anthraquinone aromatic ring fused with the imidazole heterocycle (see Figure 8). More in detail, the Hg signal shifted from 8.21 to 8.27 ppm, whereas Hf was displaced from 8.13 to 8.27 ppm. On the other hand, the protons of the biphenyl group centered at 7.90 (Hd) and 8.38 (He) ppm shifted to 8.08 and 8.51 ppm, respectively. These observed shifts are tentatively ascribed to a preferential coordination of Al^{3+} cation with one of the nitrogen atoms of the imidazole ring.

Finally, the 1:1 stoichiometry of the complex formed between probes **2a−d** and Al^{3+}, Fe^{3+}, and Cr^{3+} was assessed by the method of continuous variation (Job's plot). The Job's plot for the interaction between **2a** and Fe^{3+} cation is shown in Figure 9. In all cases, the formation of 1:1 (probe−trivalent cation) complexes was confirmed.

Stability Constants with Cations. To complete the characterization of the interaction between probes **2a−d** and cations, the corresponding stability constants for the formation of 1:1 complexes were determined from UV−visible spectroscopic titrations using the HypSpec software. The results are shown in Table 6. As shown, the stability constants determined for probes **2b**, **2c**, and **2d** were of the same order of magnitude and were in the 3.74−4.52 range. Compared with these data, **2a** formed, in general, stronger complexes with values of the logarithms of the stability constants of 5.28, 4.80, and 4.49 for the coordination with Al^{3+}, Cr^{3+}, and Fe^{3+}, respectively. The fact that **2a** forms complexes with trivalent metal cations stronger than that of **2b−d** may be tentatively ascribed to the presence of *N*-methylpyrrole, thiophene, and furan heterocycles in **2b−d** that may inhibit, to some extent, the coordination with the trivalent cations.

dx.doi.org/10.1021/jo501515e | J. Org. Chem. 2014, 79, 10752−10761

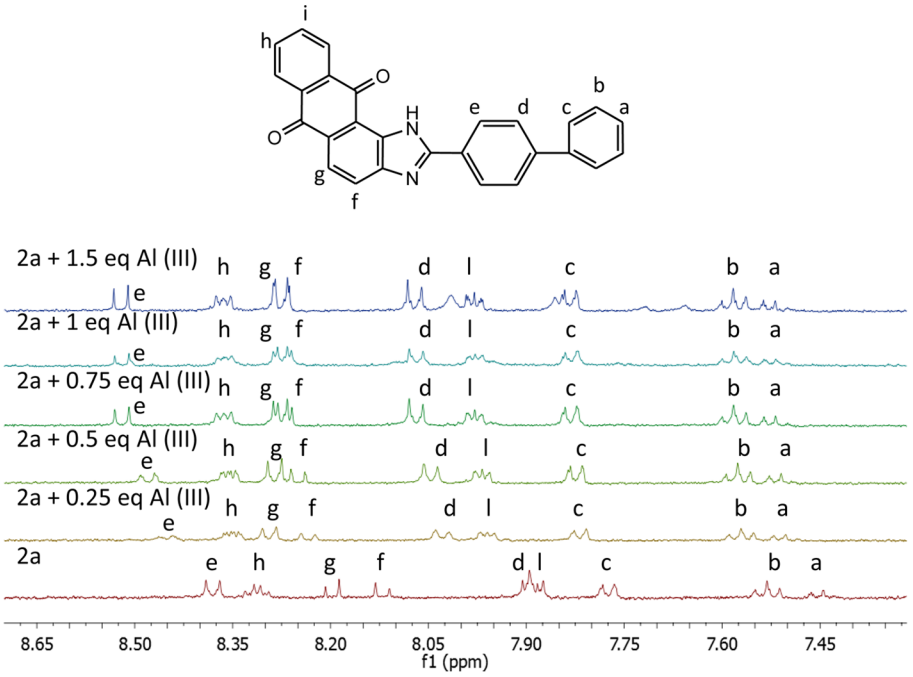

Figure 8. ^{1}H NMR spectra of probe **2a** in CD_3CN alone and in the presence of increasing quantities of Al^{3+} cation.

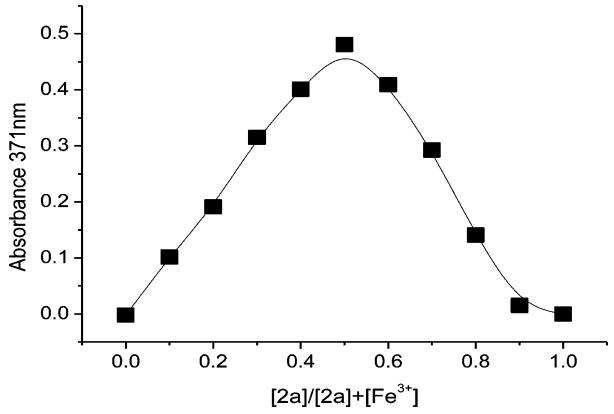

Figure 9. Job's plot for the complexation of **2a** with Fe^{3+} cation determined by UV−visible spectrophotometry in acetonitrile at 371 nm and $[\mathbf{2a}] + [Fe^{3+}] = 1.0 \times 10^{-3}$ mol dm^{-3}.

Table 6. Logarithms of the Stability Constants Calculated for the Probes 2a−d with Trivalent Cations (C^{3+} = Al^{3+}, Cr^{3+}, and Fe^{3+}) Interactions

	LH + C^{3+} ⇆ LH···C^{3+}		
	Al^{3+}	Cr^{3+}	Fe^{3+}
2a	5.28 ± 0.02	4.80 ± 0.02	4.49 ± 0.02
2b	4.44 ± 0.04	3.74 ± 0.05	4.52 ± 0.03
2c	4.23 ± 0.04	4.34 ± 0.03	4.40 ± 0.03
2d	4.52 ± 0.04	4.19 ± 0.05	4.01 ± 0.07

CONCLUSION

A family of imidazoanthraquinone probes (**2a−d**) was synthesized and characterized. Moreover, their interactions with ions were studied via UV−visible, fluorescence, and ^{1}H NMR spectroscopy. Among the anions tested, F^- induced a clear deprotonation process for **2a−d** that was reflected in a red-shift of the absorption and in a moderate quenching of the emission intensities of the four probes. Other basic anions (AcO^- and $H_2PO_4^-$) induced moderate changes in the UV−visible and emission profiles of the probes. On the other hand, of all the cations tested, only Al^{3+}, Fe^{3+}, and Cr^{3+} induced changes in the UV−visible and fluorescence of **2a−d**. In particular, addition of trivalent cations to solutions of the four probes induced a remarkable blue shift of the absorption band and a partial quenching of the emission. The spectroscopic changes observed with of Al^{3+}, Fe^{3+}, and Cr^{3+} were ascribed to the formation of 1:1 (probe−cation) complexes. ^{1}H NMR measurements suggested that trivalent cations coordinated with the donor part of the probes, i.e., the imidazole group. Receptors **2a−d** are rare dual probes that can be used as both anion (F^-) or cation (Al^{3+}, Fe^{3+}, and Cr^{3+}) chemosensors.

EXPERIMENTAL SECTION

Materials and Methods. *General.* TLC analyses were carried out on 0.25 mm thick precoated silica plates, and spots were visualized under UV light. NMR spectra were obtained at an operating frequency of 300 or 400 MHz for ^{1}H and 75.4 or 100.6 MHz for ^{13}C using the solvent peak as internal reference at 25 °C. All chemical shifts are given in ppm using δ_H Me_4Si = 0 ppm as reference, and J values are given in hertz. Precursors **1a**, **1b**, **1d**, and 1,2-diaminoanthraquinone are commercially available and were used as received.

*Synthesis of Formyl Precursor **1c**.* The synthesis of compound **1c** includes two steps: (i) Suzuki−Miyaura cross-coupling to obtain the intermediate 1-methyl-2-phenyl-1*H*-pyrrole followed by (ii) Vilsmeier formylation to obtain the formyl precursor 1-methyl-5-phenyl-1*H*-pyrrole-2-carbaldehyde.

i. Suzuki−Miyaura Cross-Coupling. To bromobenzene (0.112 g, 0.72 mmol) in DME (6 mL) were added 1-methyl-2-(4,4,5,5-tetramethyl-1,3,2-dioxaborolan-2-yl)-1*H*-pyrrole (0.193 g, 0.93 mmol, 1.3 equiv), $Pd(PPh_3)_4$ (0.050 g, 0.06 equiv), and 2 M Na_2CO_3 (0.72 mL, 2 equiv). The mixture was stirred at 80 °C under an argon atmosphere during 15 h until disappearance of the halide. The mixture was cooled to room temperature, and a saturated solution of NaCl (10 mL) and ethyl acetate (30 mL) were added. The two phases were separated, and the organic phase was extracted with ethyl acetate (3 × 20 mL), washed with water and then with aqueous NaOH (10%), dried with anhydrous magnesium sulfate, and evaporated to dryness. The obtained residue was purified by column chromatography, using

dx.doi.org/10.1021/jo501515e | J. Org. Chem. 2014, 79, 10752−10761

mixtures of diethyl ether and light petroleum ether of increasing polarity, and 1-methyl-2-phenyl-1*H*-pyrrole was obtained as a yellow oil[44] (0.085 g, 76%).

ii. Vilsmeier Formylation. $POCl_3$ (0.079 mL, 1.20 mmol) was added to DMF (0.056 mL, 1.20 mmol), and the mixture was stirred for 15 min at 0 °C. 1-Methyl-2-phenyl-1*H*-pyrrole (0.062 g, 0.39 mmol) dissolved in DMF (1 mL) was added dropwise with stirring. The mixture was heated for 2 h at 60 °C. The solution was then poured slowly into a saturated sodium acetate aqueous solution (5 mL) and stirred during 30 min. The organic layer was diluted with diethyl ether (20 mL), washed with saturated $NaHCO_3$ aqueous solution (10 mL), and dried with anhydrous $MgSO_4$. The organic extract was filtered, evaporated under reduced pressure, and purified by column chromatography, using mixtures of diethyl ether and light petroleum ether of increasing polarity, yielding 1-methyl-5-phenyl-1*H*-pyrrole-2-carbaldehyde (**1c**) as colorless oil (0.073 g, 90%).[45] ^{1}H NMR (400 MHz, $CDCl_3$) δ = 6.31 (d, 1H, J = 4.0 Hz, H-4), 6.98 (d, 1H, J = 4.0 Hz, H-3), 7.40−7.47 (m, 5H, H-2′, H-3′, H-4′, H-5′ and H-6′), 9.59 (s, 1H, C*H*O) ppm.

General Procedure for the Synthesis of Imidazoanthraquinones ***2a−d****. i. Preparation of the Imines.* The aldehydes **1a−d** (0.20 mmol) and 1,2-diaminoanthraquinone (0.24 mmol) were dissolved separately in ethanol (4 mL/mmol). The ethanolic solution of aldehyde and formic acid (0.04 mL/mmol of aldehyde) was added to the solution of 1,2-diaminoanthraquinone heated at reflux. The reaction mixture was heated under reflux overnight.

ii. Cyclization of the Imines. After cooling, the ethanolic solution was evaporated and the crude imine was dissolved in a small volume of acetic acid (5 mL/mmol of imine). To this solution was added lead tetraacetate (0.20 mmol), and the mixture was stirred overnight at room temperature. The mixture was poured into water (20 mL) and extracted with chloroform (2 × 50 mL). The organic layer was dried with magnesium sulfate and evaporated under reduced pressure to give compounds **2a−d**, which were purified by column chromatography on silica with chloroform as eluent.

*2-([1′,1″-Biphenyl]-4′-yl)-1H-anthra[1,2-d]imidazole-6,11-dione (**2a**).* Yellow solid (55 mg, 65%). Mp: 267−269 °C (269−270 °C[46]). ^{1}H NMR (400 MHz, DMSO-d_6) δ = 7.40−7.44 (m, 1H), 7.49−7.53 (m, 2H), 7.79 (dd, 2H, J = 8.4 and 1.2 Hz), 7.87 (d, 2H, J = 8.4 Hz), 7.91−7.95 (m, 2H), 8.07−8.14 (m, 2H), 8.19−8.24 (m, 2H), 8.52 (d, 2H, J = 8.0 Hz), 13.23 (s, 1H) ppm.

*2-(5′-Phenylthiophen-2′-yl)-1H-anthra[1,2-d]imidazole-6,11-dione (**2b**).* Orange solid (53 mg, 71%). Mp: 269−271 °C. ^{1}H NMR (300 MHz, DMSO-d_6) δ = 7.34−7.39 (m, 1H), 7.43−7.48 (m, 2H), 7.63 (d, 1H, J = 3.9 Hz), 7.74 (d, 2H, J = 7.2 Hz), 7.86−7.93 (m, 2H), 8.02 (s, 2H), 8.15−8.21 (m, 2H), 8.50 (d, 1H, J = 3.9 Hz), 13.38 (s, 1H) ppm. ^{13}C NMR (75.4 MHz, DMSO-d_6) δ = 118.3, 121.2, 124.3, 125.2, 125.7, 126.2, 126.8, 127.9, 128.6, 129.3, 131.3, 131.6, 132.8, 132.9, 133.0, 133.1, 134.2, 134.4, 147.4, 149.2, 152.7, 182.2, 183.1 ppm. MS (FAB) m/z (%): 407 ([M + H]$^+$, 25), 406 (M$^+$, 9), 307 (33), 289 (17), 166 (13), 155 (30), 154 (100). HRMS: (FAB) m/z (%) for $C_{25}H_{15}N_2O_2S$; calcd 407.0854; found 407.0847.

*2-(1′-Methyl-5′-phenyl-1H-pyrrol-2′-yl)-1H-anthra[1,2-d]-imidazole-6,11-dione (**2c**).* Dark red solid (24 mg, 32%). Mp: 246−248 °C. ^{1}H NMR (400 MHz, DMSO-d_6) δ = 4.08 (s, 3H), 6.39 (d, 1H, J = 4.0 Hz), 7.39−7.44 (m, 1H), 7.48−7.56 (m, 4H), 7.59 (d, 1H, J = 4.0 Hz), 7.88−7.93 (m, 2H), 8.04 (s, 2H), 8.19−8.24 (m, 2H), 12.74 (s, 1H) ppm. ^{13}C NMR (100.6 MHz, DMSO-d_6) δ = 35.2, 109.8, 115.5, 117.7, 121.0, 123.3, 123.8, 126.2, 126.8, 127.3, 127.8, 128.7, 128.9, 131.9, 132.3, 133.1, 133.3, 134.2, 134.4, 140.2, 149.8, 152.3, 182.2, 183.2 ppm. HRMS: (FAB) m/z (%) for $C_{26}H_{17}N_3O_2$; calcd 403.1321; found 403.1307.

*2-(5′-Phenylfuran-2′-yl)-1H-anthra[1,2-d]imidazole-6,11-dione (**2d**).* Dark orange solid (38 mg, 33%). Mp: 250−252 °C. ^{1}H NMR (400 MHz, DMSO-d_6) δ = 7.22 (d, 1H, J = 4.0 Hz), 7.38 (t, 1H, J = 8.0 Hz), 7.50 (t, 2H, J = 8.0 Hz), 7.84 (d, 1H, J = 4.0 Hz), 7.87−7.89 (m, 2H), 7.94 (d, 2H, J = 8.0 Hz), 8.01−8.06 (m, 2H), 8.15−8.19 (m, 2H), 13.27 (s, 1H) ppm. ^{13}C NMR (100.6 MHz, DMSO-d_6) δ = 108.5, 116.7, 118.5, 121.2, 124.3, 124.6, 126.2, 126.8, 128.0, 128.6, 129.0, 129.3, 132.4, 133.0, 133.1, 134.2, 134.5, 143.6, 149.1, 149.5, 155.7, 182.2, 183.1 ppm. HRMS: (FAB) m/z (%) for $C_{25}H_{14}N_2O_3$; calcd 390.1004; found 390.0986.

Physical Measurements. Stock solutions of the anions (F^-, Cl^-, Br^-, I^-, OCN^-, BzO^-, ClO_4^-, AcO^-, HSO_4^-, $H_2PO_4^-$, and CN^- as tetrabutylammonium salts) and cations ($Cu(ClO_4)_2{\cdot}6H_2O$, $Co(ClO_4)_2{\cdot}6H_2O$, $Mg(ClO_4)_2$, $Fe(ClO_4)_3{\cdot}xH_2O$, $Ba(ClO_4)_2$, $Fe(ClO_4)_2{\cdot}xH_2O$, $Ni(ClO_4)_2{\cdot}6H_2O$, $Ca(ClO_4)_2{\cdot}4H_2O$, $Zn(ClO_4)_2{\cdot}6H_2O$, $Pb(ClO_4)_2{\cdot}xH_2O$, $Cd(ClO_4)_2{\cdot}xH_2O$, $Cr(ClO_4)_3{\cdot}6H_2O$, $Al(ClO_4)_3{\cdot}9H_2O$, $KClO_4$, and $LiClO_4$) were prepared at 10^{-3} mol dm^{-3} in acetonitrile. The concentrations of ligands used in spectroscopy measurements were ca. 1×10^{-4} and 1×10^{-5} mol dm^{-3}. The quantity of anion solutions added did not exceed 10% of the volume of the compounds **2a−d** to avoid relevant changes in the total solution concentration. For the probes that required the addition of excess of ions (30 equiv), corrections of the volume and concentration were made. The UV−vis and fluorescence titrations were measured at room temperature (25 °C).

Theoretical Studies. Quantum chemical calculations were carried out in vacuum with Hyperchem V6.03 with a semiempirical level (PM3, within restricted Hartree−Fock level). For optimization, the Polar−Ribiere algorithm was used. The convergence limit and the RMS gradient were set to 0.01 kcal mol^{-1}. Stability constants were calculated with the HypSpec Software V1.1.18 and using the data of the titration of receptors with target anions and cations.

■ ASSOCIATED CONTENT

Supporting Information

^{1}H NMR spectra of compounds **1c** and **2a**, ^{1}H and ^{13}C spectra of probes **2b−d**. UV−vis and emission titration profiles. Cartesian coordinates of the optimized geometries. This material is available free of charge via the Internet at http://pubs.acs.org.

■ AUTHOR INFORMATION

Corresponding Authors

*E-mail: rmaez@qim.upv.es.

*E-mail: mfox@quimica.uminho.pt.

Notes

The authors declare no competing financial interest.

■ ACKNOWLEDGMENTS

We thank the Spanish Government (project MAT2012-38429-C04) for support. C. Marín-Hernández thanks the Spanish Ministry of Economy and Competitiveness for her grant. We also gratefully acknowledge financial support from Fundación Carolina and UPNFM-Honduras for a predoctoral grant to L. E. Santos-Figueroa and from Spanish Ministry of Science and Innovation for a FPU grant to M. E. Moragues. Thanks are also given to the Fundação para a Ciência e Tecnologia (Portugal) and FEDER-COMPETE for financial support through the Centro de Química - Universidade do Minho, Project PEst-C/QUI/UI0686/2013 (FCOMP-01-0124-FEDER-037302) and a Postdoctoral grant to R.M.F. Batista (SFRH/BPD/79333/2011). We are also grateful to the Instituto da Educação of Universidade do Minho for providing the laboratory infrastructure necessary for the development of this work.

■ REFERENCES

(1) Kaur, K.; Saini, R.; Kumar, A.; Luxami, V.; Kaur, N.; Singh, P.; Kumar, S. *Coord. Chem. Rev.* **2012**, *256*, 1992−2028.

(2) (a) Rurack, K. *Spectrochim. Acta, Part A* **2001**, *57A*, 2161−2195. (b) Lloris, J. M.; Martñinez-Máñez, R.; Padilla-Tosta, M. E.; Pardo, T.; Soto, J.; Beer, P. D.; Cadman, J.; Smith, D. K. *J. Chem. Soc., Dalton Trans.* **1999**, *14*, 2359−2369.

(3) Miyaji, H.; Sessler, J. L. *Angew. Chem., Int. Ed.* **2001**, *40*, 154−157.

(4) (a) Yuan, L.; Lin, W.; Zheng, K.; Zhu, S. *Acc. Chem. Res.* **2013**, *46*, 1462−1473. (b) Doussineau, T.; Schulz, A.; Lapresta-Fernandez, A.; Moro, A.; Körsten, S.; Trupp, S.; Mohr, G. J. *Chem.—Eur. J.* **2010**, *16*, 10290−10299. (c) Wang, S.; Li, N.; Pan, W.; Tang, B. *Trends Anal. Chem.* **2012**, *39*, 3−37.
(5) See for example: (a) Kaur, N.; Kumar, S. *Tetrahedron* **2011**, *67*, 9233−9264. (b) Prodi, L.; Montalti, M.; Zaccheroni, N.; Dolci, L. S. *Top. Fluoresc. Spectrosc.* **2005**, *9*, 1−57. (c) Fabbrizzi, L.; Poggi, A. *Chem. Soc. Rev.* **1995**, *24*, 197−202. (d) Okamoto, K.; Araki, Y.; Ito, O.; Fukuzumi, S. *J. Am. Chem. Soc.* **2004**, *126*, 56−57. (e) Okamoto, K.; Fukuzumi, S. *J. Am. Chem. Soc.* **2004**, *126*, 13922−13923.
(6) (a) Suksai, C.; Tuntulani, T. *Chem. Soc. Rev.* **2003**, *32*, 192−202. (b) Snowden, T. S.; Ansyn, E. V. *Curr. Opin. Chem. Biol.* **1999**, *3*, 740−746. (c) Wiskur, S. L.; Ait-Haddou, H.; Lavigne, J. J.; Anslyn, E. V. *Acc. Chem. Res.* **2001**, *34*, 963−972. (d) Fukuzumi, S.; Ohkubo, K.; D'Souza, F.; Sessler, J. L. *Chem. Commun.* **2012**, *48*, 9801−9815.
(7) Beer, P. D.; Gale, P. A. *Angew. Chem., Int. Ed.* **2001**, *40*, 486−516.
(8) (a) Santos-Figueroa, L. E.; Moragues, M. E.; Climent, E.; Agostini, A.; Martínez-Máñez, R.; Sancenón, F. *Chem. Soc. Rev.* **2013**, *42*, 3489−3613. (b) Moragues, M. E.; Martínez-Máñez, R.; Sancenón, F. *Chem. Soc. Rev.* **2011**, *40*, 2593−2643.
(9) Martínez-Máñez, R.; Sancenón, F. *Chem. Rev.* **2003**, *103*, 4419−4476.
(10) (a) Schug, K. A.; Lindner, W. *Chem. Rev.* **2005**, *105*, 67−113. (b) Blondeau, P.; Segura, M.; Pérez-Fernández, R.; de Mendoza, J. *Chem. Soc. Rev.* **2007**, *36*, 198−210. (c) Gale, P. A.; García-Garrido, S. E.; Garric, J. *Chem. Soc. Rev.* **2008**, *37*, 151−190. (d) Steed, J. W. *Chem. Soc. Rev.* **2009**, *38*, 506−519.
(11) (a) Dydio, P.; Lichosyt, D.; Jurczak, J. *Chem. Soc. Rev.* **2011**, *40*, 2971−2985. (b) Sessler, J. L.; Camiolo, S.; Gale, P. A. *Coord. Chem. Rev.* **2003**, *240*, 17−55. (c) Bondy, C. R.; Loeb, S. J. *Coord. Chem. Rev.* **2003**, *240*, 77−99. (d) Choi, K.; Hamilton, A. D. *Coord. Chem. Rev.* **2003**, *240*, 101−110.
(12) (a) Yoon, J.; Kim, S. K.; Singh, N. J.; Kim, K. S. *Chem. Soc. Rev.* **2006**, *35*, 355−360. (b) Xu, Z.; Kim, S. K.; Yoon, J. *Chem. Soc. Rev.* **2010**, *39*, 1457−1466.
(13) (a) Raposo, M. M. M.; García-Acosta, B.; Ábalos, T.; Calero, P.; Martínez-Máñez, R.; Ros-Lis, J. V.; Soto, J. *J. Org. Chem.* **2010**, *75*, 2922−2933. (b) Santos-Figueroa, L. E.; Moragues, M. E.; Raposo, M. M. M.; Batista, R. M. F.; Costa, S. P. G.; Ferreira, R. C. M.; Sancenón, F.; Martínez-Máñez, R.; Ros-Lis, J. V.; Soto, J. *Org. Biomol. Chem.* **2012**, *10*, 7418−7428.
(14) Winter, W. E.; Bazydlo, L. A.; Harris, N. S. *Lab. Med.* **2014**, *45*, 92−102.
(15) von Haehling, S.; Anker, S. D. *Dtsch. Med. Wochenschr.* **2014**, *139*, 841−844.
(16) (a) Perl, D.; Brody, A. *Science* **1980**, *208*, 297−299. (b) Belojevic, G.; Jakovljevic, B. *Srp. Arh. Celok. Lek.* **1998**, *126*, 283−289. (c) Perl, D.; Gajdusek, D.; Garruto, R.; Yanagihara, R.; Gibbs, C. *Science* **1982**, *217*, 1053−1055.
(17) Mertz, W. *J. Nutr.* **1993**, *123*, 626−633.
(18) Wallach, S. *J. Am. Coll. Nutr.* **1985**, *4*, 107−120.
(19) Szczygiel, J.; Dyrek, K.; Kruczala, K.; Bidzinska, E.; Brozek-Mucha, Z.; Wenda, E.; Wieczorek, J.; Szymonska, J. *J. Phys. Chem. B* **2014**, *118*, 7100−7107.
(20) (a) Langdon-Jones, E. E.; Pope, S. J. A. *Coord. Chem. Rev.* **2014**, *269*, 32−53. (b) Batista, R. M. F.; Costa, S.P. G.; Raposo, M. M. M. *Sens. Actuators, B* **2014**, *191*, 791−799. (c) Batista, R. M. F.; Oliveira, E.; Costa, S. P. G.; Lodeiro, C.; Raposo, M. M. M. *Supramol. Chem.* **2014**, *26*, 71−80. (d) Saini, R.; Kaur, N.; Kumar, S. *Tetrahedron* **2014**, *70*, 4285−4307.
(21) (a) Stathopoulou, K.; Valianou, L.; Skaltsounis, A.-L.; Karapanagiotis, I.; Magiatis, P. *Anal. Chim. Acta* **2013**, *804*, 264−272. (b) Shindy, H. A. *Mini-Rev. Org. Chem.* **2012**, *9*, 361−373.
(22) (a) De Almeida, D. P.; Gomide, J. L. *Papel* **2013**, *74*, 53−56. (b) Song, W.; Liu, J. *J. Chem. Pharm. Res.* **2013**, *5*, 1217−1221. (c) Alfaro, A.; López, F.; Pérez, A.; García, J. C.; Pelach, M. A.; Mutje, P. *Cell. Chem. Technol.* **2013**, *47*, 765−775.
(23) (a) Chen, M.; Zhang, C.; Shen, Y.; Zu, G. *Adv. Mater. Res.* **2013**, *610−613*, 9−14. (b) Gomes, A. C.; Nunes, J. C.; Simoes, R. M. S. *J. Hazard. Mater.* **2010**, *178*, 57−65.
(24) (a) Zhu, H.; Yang, Y.; Hyeon-Deuk, K.; Califano, M.; Song, N.; Wang, Y.; Zhang, W.; Prezhdo, O. V.; Lian, T. *Nano Lett.* **2014**, *14*, 1263−1269. (b) Rabache, V.; Chaste, J.; Petit, P.; Della Rocca, M. L.; Martin, P.; Lacroix, J.-C.; McCreery, R. L.; Lafarge, P. *J. Am. Chem. Soc.* **2013**, *135*, 10218−10221. (c) Darwish, N.; Díez-Pérez, I.; Da Silva, P.; Tao, N.; Gooding, J. J.; Paddon-Row, M. N. *Angew. Chem., Int. Ed.* **2012**, *51*, 3203−3206.
(25) (a) Liu, Z.; Wei, F.; Chen, L.-J.; Xiong, H.-R.; Liu, Y.-Y.; Luo, F.; Hou, W.; Xiao, H.; Yang, Z.-Q. *Molecules* **2013**, *18*, 11842−11858. (b) Li, D.; Zhang, N.; Cao, Y.; Zhang, W.; Su, G.; Sun, Y.; Liu, Z.; Li, F.; Liang, D.; Liu, B.; Guo, M.; Fu, Y.; Zhang, X.; Yang, Z. *Eur. J. Pharmacol.* **2013**, *705*, 79−85.
(26) (a) Claes, P.; Cappoen, D.; Uythethofken, C.; Jacobs, J.; Mertens, B.; Mathys, V.; Verschaeve, L.; Huygen, K.; De Kimpe, N. *Eur. J. Med. Chem.* **2014**, *77*, 409−421. (b) Yildiz, E.; Keles, M.; Kaya, A.; Dincer, S. *Chem. Sci. Trans.* **2013**, *2*, 547−555. (c) Kardong, D.; Upadhyaya, S.; Salkia, L. R. *J. Pharm. Res.* **2013**, *6*, 179−182.
(27) Patil, A. G.; Joshi, K. A.; Patil, D. A.; Phatak, A. V.; Naresh, C. *Pharmacogn. J.* **2009**, *1*, 267−272.
(28) (a) Ayo, R. G. *J. Med. Plants Res.* **2010**, *4*, 1339−1348. (b) Ee, G. L. C.; Ng, K. N. *Asian J. Chem.* **2004**, *16*, 429−433.
(29) (a) Shah, A.; Varma, O.; Patankar, S.; Kadam, V. *Curr. Bioact. Compd.* **2013**, *9*, 288−305. (b) Khamthong, N.; Rukachaisirikul, V.; Phongpaichit, S.; Preedanon, S.; Sakayaroj, J. *Tetrahedron* **2012**, *68*, 8245−8250.
(30) (a) Abdissa, N.; Induli, M.; Akala, H. M.; Heydenreich, M.; Midiwo, J. O.; Ndakala, A.; Yenesew, A. *Phytochem. Lett.* **2013**, *6*, 241−245. (b) Choomuenwai, V.; Andrews, K. T.; Davis, R. A. *Bioorg. Med. Chem.* **2012**, *20*, 7167−7174.
(31) (a) Shrestha, J. P.; Fosso, M. Y.; Bearss, J.; Chang, C.-W. T. *Eur. J. Med. Chem.* **2014**, *77*, 96−102. (b) Wei, W.-T.; Lin, S.-Z.; Liu, D.-L.; Wang, Z.-H. *Oncol. Rep.* **2013**, *30*, 2555−2562.
(32) See for example: (a) Agostini, A.; Campos, I.; Milani, M.; Elsayed, S.; Pascual, L.; Martínez-Máñez, R.; Licchelli, M.; Sancenón, F. *Org. Biomol. Chem.* **2014**, *12*, 1871−1874. (b) Climent, E.; Mondragón, L.; Martínez-Máñez, R.; Sancenón, F.; Marcos, M. D.; Murguía, J. R.; Amorós, P.; Rurack, K.; Pérez-Payá, E. *Angew. Chem., Int. Ed.* **2013**, *52*, 8939−8942. (c) Santos-Figueroa, L. E.; Giménez, C.; Agostini, A.; Aznar, E.; Marcos, M. D.; Sancenón, F.; Martínez-Máñez, R.; Amorós, P. *Angew. Chem., Int. Ed.* **2013**, *52*, 13712−13716. (d) Climent, E.; Gröninger, D.; Hecht, M.; Walter, M. A.; Martínez-Máñez, R.; Weller, M. G.; Sancenón, F.; Amorós, P.; Rurack, K. *Chem.—Eur. J.* **2013**, *19*, 4117−4122. (e) Moragues, M. E.; Esteban, J.; Ros-Lis, J. V.; Martínez-Máñez, R.; Marcos, M. D.; Martínez, M.; Soto, J.; Sancenón, F. *J. Am. Chem. Soc.* **2011**, *133*, 15762−15772. (f) Climent, E.; Marcos, M. D.; Martínez-Máñez, R.; Sancenón, F.; Soto, J.; Rurack, K.; Amorós, P. *Angew. Chem., Int. Ed.* **2009**, *48*, 8519−8522.
(33) Saha, S.; Ghosh, A.; Mahato, P.; Mishra, S.; Mishra, S. K.; Suresh, E.; Das, S.; Das, A. *Org. Lett.* **2010**, *12*, 3406−3409.
(34) Amendola, V.; Esteban-Gómez, D.; Fabbrizzi, L.; Licchelli, M. *Acc. Chem. Res.* **2006**, *39*, 343−353.
(35) (a) Moragues, M. E.; Santos-Figueroa, L. E.; Ábalos, T.; Sancenón, F.; Martínez-Máñez, R. *Tetrahedron Lett.* **2012**, *53*, 5110−5113. (b) Batista, R. M. F.; Oliveira, E.; Costa, S. P. G.; Lodeiro, C.; Raposo, M. M. M. *Tetrahedron* **2011**, *67*, 7106−7113. (c) Santos-Figueroa, L. E.; Moragues, M. E.; Batista, R. M. F.; Costa, S. P. G.; Raposo, M. M. M.; Ferreira, R. C. M.; Sancenón, F.; Martínez-Máñez, R.; Ros-Lis, J. V.; Soto, J. *Tetrahedron* **2012**, *68*, 7179−7186. (d) Aldrey, A.; Núñez, C.; García, V.; Bastida, R.; Lodeiro, C.; Macías, A. *Tetrahedron* **2010**, *66*, 9223−9230. (e) Atta, A. K.; Ahn, I.-H.; Hong, A.-Y.; Heo, J.; Kim, C. K.; Cho, D.-G. *Tetrahedron Lett.* **2012**, *53*, 575−578. (f) Amendola, V.; Fabbrizzi, L.; Mosca, L.; Schmidtchen, F.-P. *Chem.—Eur. J.* **2011**, *17*, 5972−5981. (g) Amendola, V.; Bergamaschi, G.; Boiocchi, M.; Fabbrizzi, L.; Milani, M. *Chem.—Eur. J.* **2010**, *16*, 4368−4380.

(36) Bordwell, F. G. *Acc. Chem. Res.* **1988**, *21*, 456−463. The pK_a of acetic and hydrofluoric acids in DMSO are 12.3 and 15.2, respectively. Taking into account this value, fluoride is a stronger base than acetate in organic solvents and the extension of the proton shift observed with the former anion is larger than that observed for the latter.
(37) Batista, R. M: F.; Oliveira, E.; Costa, S. P. G.; Lodeiro, C.; Raposo, M. M. M. *Org. Lett.* **2007**, *9*, 3201−3204.
(38) Peng, X.; Wu, Y.; Fan, J.; Tian, M.; Han, K. *J. Org. Chem.* **2005**, *70*, 10524−10531.
(39) Li, G.-Y.; Zhao, G.-J.; Liu, Y.-H.; Han, K.-L.; He, G. Z. *J. Comput. Chem.* **2010**, *31*, 1759−1765.
(40) *HyperChem 6.03 Molecular Modeling System*, Hypercube Inc., Gainesville, FL.
(41) (a) Kumari, N.; Jha, S.; Bhattacharya, S. *J. Org. Chem.* **2011**, *76*, 8215−8222. (b) Batista, R. M. F.; Costa, S. P. G.; Raposo, M. M. M. *J. Photochem. Photobiol., A* **2013**, *259*, 33−40.
(42) (a) Chawla, H. M.; Shukla, R.; Shubha, P. *Tetrahedron Lett.* **2012**, *53*, 2996−2999. (b) Yang, H.; Zhou, Z.-G.; Xu, J.; Li, F.-Y.; Yi, T.; Huang, C.-H. *Tetrahedron* **2007**, *63*, 6732−6736. (c) Yoshida, K.; Mori, T.; Watanabe, S.; Kawai, H.; Nagamura, T. *J. Chem. Soc., Perkin Trans. 2* **1999**, 393−398.
(43) Valeur, B.; Leray, I. *Coord. Chem. Rev.* **2000**, *205*, 3−40.
(44) Wen, J.; Qin, S.; Ma, L.-F.; Dong, L.; Zhang, J.; Liu, S.-S.; Duan, Y.-S.; Chen, S.-Y.; Hu, C.-W.; Yu, X.-Q. *Org. Lett.* **2010**, *12*, 2694−2697.
(45) Carson, J. R.; Jetter, M. C.; Lee, J. S.; Youngman M. A. U.S. Patent Appl. 20040192720 A1 20040930, 2004.
(46) da Silva, E. N.; Guimaraes, T. T.; Menna-Barreto, R. R. S.; Pinto, M. D. F. R.; de Simone, C. A.; Pessoa, C.; Cavalcanti, B. C.; Sabino, J. R.; Andrade, C. K. Z.; Goulart, M. O. F.; de Castro, S. L.; Pinto, A. V. *Bioorg. Med. Chem.* **2010**, *18*, 3224−3230.